Elliptic (v_2) and triangular (v_3) anisotropic flow of identified hadrons from the STAR Beam Energy Scan program

P. Parfenov (for the STAR Collaboration)

National Research Nuclear University MEPhI (Moscow Engineering Physics Institute), Kashirskoe highway 31, Moscow, 115409, Russia

E-mail: PEParfenov@mephi.ru

Abstract.

Elliptic (v_2) and triangular (v_3) anisotropic flow coefficients for inclusive and identified charged hadrons ($\pi^{\pm}$, $K^{\pm}$, p, $\bar{p}$) at midrapidity in Au+Au collisions, measured by the STAR experiment in the Beam Energy Scan (BES) at the Relativistic Heavy Ion Collider at $\sqrt{s_{NN}}$ = 11.5 - 62.4 GeV, are presented. We observe that the triangular flow signal (v_3) of identified hadrons exhibits similar trends as first observed for v_2 in Au+Au collisions, i.e. (i) mass ordering at low transverse momenta, $p_T < 2$ GeV/c, (ii) meson/baryon splitting at intermediate p_T, $2 < p_T < 4$ GeV/c, and (iii) difference in flow signal of protons and antiprotons. New measurements of v_3 excitation function could serve as constraints to test different models and to aid new information about the temperature dependence of the transport properties of the strongly interacting matter.

1. Introduction

The heavy-ion experiments at the Relativistic Heavy Ion Collider (RHIC) and the Large Hadron Collider (LHC) have established the existence of a strongly coupled Quark Gluon Plasma [1, 2], a new state of QCD matter with partonic degrees of freedom and with low specific shear viscosity η/s [3]. Lattice QCD calculations [4] indicate that the quark-hadron transition is a smooth crossover at top RHIC energy and above (at high temperatures T and small values of baryonic chemical potential μ_B). A Beam Energy Scan (BES) program at RHIC plays a central role in the experimental study of the QCD phase diagram over a wide range in T and μ_B [5, 6].

The anisotropic flow is one of the important observables sensitive to the equation of state (EOS) and transport properties of the strongly interacting matter such as the shear viscosity over entropy ratio η/s [3, 7, 8]. The azimuthal anisotropy of produced particles can be quantified by the Fourier coefficients v_n in the expansion of the particles azimuthal distribution as: $dN/d\phi \propto 1 + \sum_{n=1} 2v_n \cos(n(\phi - \Psi_n))$ [7, 9], where n is the order of the harmonic, ϕ is the azimuthal angle of particles for a given type, and Ψ_n is the azimuthal angle of the nth-order event plane. The n^{th}-order flow coefficients v_n can be calculated as $v_n = \langle\cos[n(\varphi - \Psi_n)]\rangle$, where the brackets denote an average over particles and events. Elliptic (v_2) and triangular (v_3) flows are the dominant flow signals and have been studied very extensively both at top RHIC and LHC energies [10, 11, 12]. For low transverse momentum ($p_T <$ 2-3 GeV/c), the p_T dependence of v_2 and v_3 for produced particles is well described by viscous hydrodynamic models and a good agreement between data and model calculations can be reached for the small values of η/s close to the lower conjectured bound of $1/4\pi$ [3]. The shear viscosity suppresses triangular flow signal v_3 more strongly than elliptic flow signal v_2 [13, 14]. The data for top RHIC energy show that, for a given collision centrality, the measured values of v_n ($n = 2, 3$) for all hadrons scale to a single curve when plotted as $v_n/n_q^{n/2}$ versus scaled transverse kinetic energy, $(m_T - m_0)/n_q$, where n_q is the number of constituent quarks in the hadron and m_0 is mass [10, 11]. The observed empirical Number-of-Constituent Quark (NCQ) scaling with transverse kinetic energy may indicate that the bulk of the anisotropic flow at top RHIC energies is partonic, rather than hadronic [15]. The collision energy dependence of elliptic flow (v_2) for inclusive and identified hadrons at mid-rapidity in Au+Au collisions, has been studied very extensively by STAR experiment at $\sqrt{s_{NN}}$ = 7.7 - 62.4 GeV [16, 17, 18, 19]. The elliptic flow signal $v_2(p_T)$ for inclusive charged hadrons shows a very small change over such a wide range of collision energies [16]. Hybrid model calculations show that the weak dependence of $v_2(p_T)$ on the beam energy may result from the interplay of the hydrodynamic and hadronic transport phase [14]. The triangular flow v_3 is expected to be more sensitive to the viscous damping and might be an ideal observable to probe the formation of a QGP at different collision energies [20]. However, a significant difference in the v_2 values between particles and the corresponding anti-particles was observed [18, 19]. This difference increases with decreasing collision energy and is larger for baryons than mesons. Several different theoretical models have been proposed for the possible physical reason for this effect and new measurements of v_3 for particles and anti-particles might be important for distinguishing between them [18, 19]. In this work, we report new measurements of triangular (v_3) anisotropic flow coefficients for inclusive and identified charged hadrons ($\pi^{\pm}$, $K^{\pm}$, p, $\bar{p}$) at midrapidity in Au+Au collisions at $\sqrt{s_{NN}}$ = 11.5 - 62.4 GeV and compare them to v_2 results.

2. Data Analysis

The data reported in this analysis are from Au+Au collisions at $\sqrt{s_{NN}}$ = 11.5, 14.5, 19.6, 27, 39 and 62.4 GeV, collected during the beam energy scan phase-I and II (BES-I & BES-II) programs by the STAR detector using a minimum bias trigger. The collision vertices were reconstructed using charged-particle tracks measured in the Time Projection Chamber (TPC). The TPC covers the full azimuth and has a pseudorapidity range of $|\eta| < 1.0$.

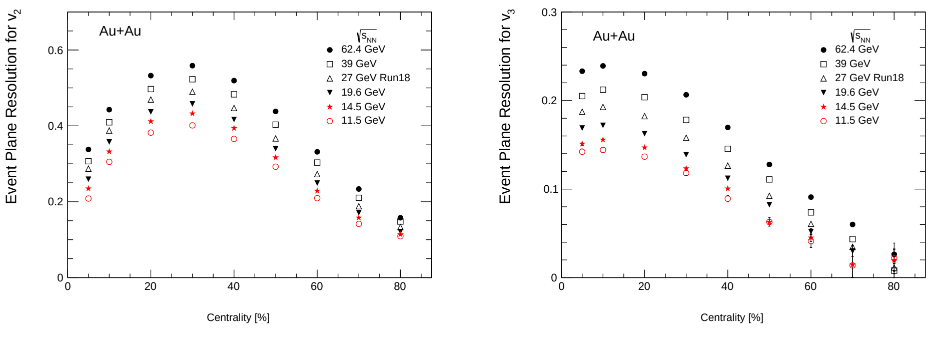

Figure 1. The centrality dependence of the event plane resolution for v_2 (left panel) and v_3 (right panel) for all six collision energies.

Events were selected to have a vertex position about the nominal center of the TPC in the beam direction of ± 40 cm at $\sqrt{s_{NN}}$ = 62, 39, 27, 19.6 and 14.5 GeV, ± 50 cm at $\sqrt{s_{NN}}$ = 11.5 GeV, and to be within a radius of $1 - 2$ cm with respect to the beam axis. The centrality of each collisions was determined by measuring event-by-event multiplicity and interpreting the measurement with a tuned Monte Carlo Glauber calculation [16, 18]. Analyzed

tracks were required to have a distance of closest approach to the primary vertex to be less than 3 cm, and to have at least 15 TPC space points used in their reconstruction [16, 17]. The particle identification for charged hadrons ($\pi^{\pm}$, $K^{\pm}$, p, $\bar{p}$) was based on a combination of the ionization energy loss, dE/dx, in the TPC, and the squared mass, m^2, from the TOF detector [17, 18, 19].
In this study, the event plane method with η sub-events, separated by an additional η-gap of $\Delta\eta > 0.1$, was used to measure elliptic (v_2) and triangular (v_3) flow [16]. The η gap is introduced to suppress the non-flow correlations between the two sub-events. The η sub-event method was implemented using the procedure in Ref [16, 17, 18]. The centrality dependence of event plane resolution for v_2 and v_3 for the six collision energies is shown in the Fig. 1. The systematic uncertainty associated with the non-flow effects is estimated for each collision energy by comparing v_2 and v_3 results obtained with different $\Delta\eta$ gaps. Studies were performed for $\Delta\eta$ values of 0.1, 0.3, 0.5, 0.7.

3. Results

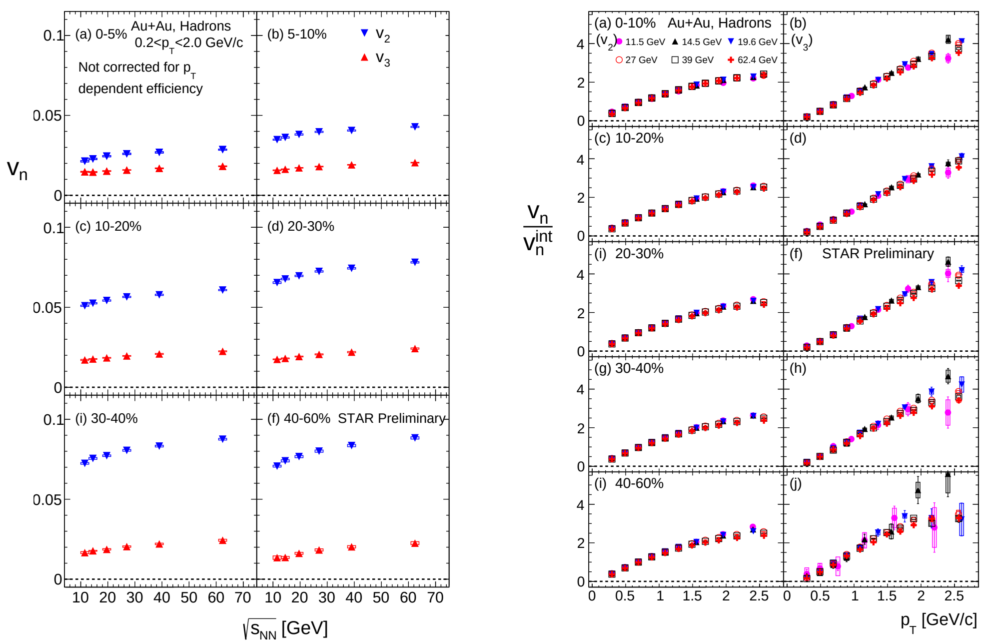

Figure 2. Left: p_T-integrated v_2^{int} and and v_3^{int} of inclusive charged hadrons as a function of $\sqrt{s_{NN}}$ for different bins in collision centrality. Right: p_T-dependence of $v_2(p_T)/v_2^{\text{int}}$ and $v_3(p_T)/v_3^{\text{int}}$ of charged hadrons for different bins in collision centrality. The measured $v_n(p_T)$ values were divided by the corresponding v_n^{int} values from the left part of the figure. The results are presented for all 6 collision energies: $\sqrt{s_{NN}} = 11.5$, 14.5, 19.6, 27, 39 and 62.4 GeV.

Preliminary results for the excitation functions of p_T-integrated ($0.2 < p_T < 3.2$ GeV/c) values of v_2^{int} and v_3^{int} of inclusive charged hadrons are presented in the left part of Fig. 2. The v_n^{int} results were not corrected for p_T dependent tracking efficiency, which will be explored in future analysis. Although the efficiency is p_T dependent but is similar between different collision energy, so it is not expected to influence the $\sqrt{s_{NN}}$ trend. The results are presented for 6 bins in collision centrality: $0-5\%$, $5-10\%$, $10-20\%$, $20-30\%$, $30-40\%$ and $40-60\%$. The results indicate an essentially monotonic increase for p_T-integrated v_2 and v_3 with $\sqrt{\mathrm{s}_{\mathrm{NN}}}$, as expected from increase of the radial flow with collision energy which pushes the hadrons to larger p_T

and renders the momentum spectra less anisotropic at low p_T [20]. The p_T dependence of $v_2(p_T)/v_2^{\rm int}$ and $v_3(p_T)/v_3^{\rm int}$ for inclusive charged hadrons is presented in the right part of the Fig. 2 for different bins in collision centrality. The measured $v_n(p_T)$ values were divided by the corresponding p_T-integrated $v_n^{\rm int}$ values from the left part of the Fig. 2. The results in the figure are presented for all 6 collision energies: $\sqrt{s_{NN}}$ = 11.5, 14.5, 19.6, 27, 39 and 62.4 GeV and they show that $v_n(p_T)/v_n^{\rm int}$ has a very week dependence on $\sqrt{\rm s_{NN}}$. This is in agreement with predictions from [21].
Figure 3 shows the collision energy dependence in $v_2(p_T)$ and $v_3(p_T)$ for identified hadrons ($\pi^{\pm}$, $K^{\pm}$, p, $\bar{p}$) for 0-60% central Au+Au collisions. The results for particles (left panel) and anti-particles (right panel) are presented separately. We observe that the $v_3(p_T)$ signal of identified charged hadrons exhibits similar trends as first observed for v_2 in Au+Au collisions: mass ordering at low transverse momenta, $p_T < 2$ GeV/c, and meson/baryon splitting at intermediate p_T, $2 < p_T < 4$ GeV/c [17, 18, 19].

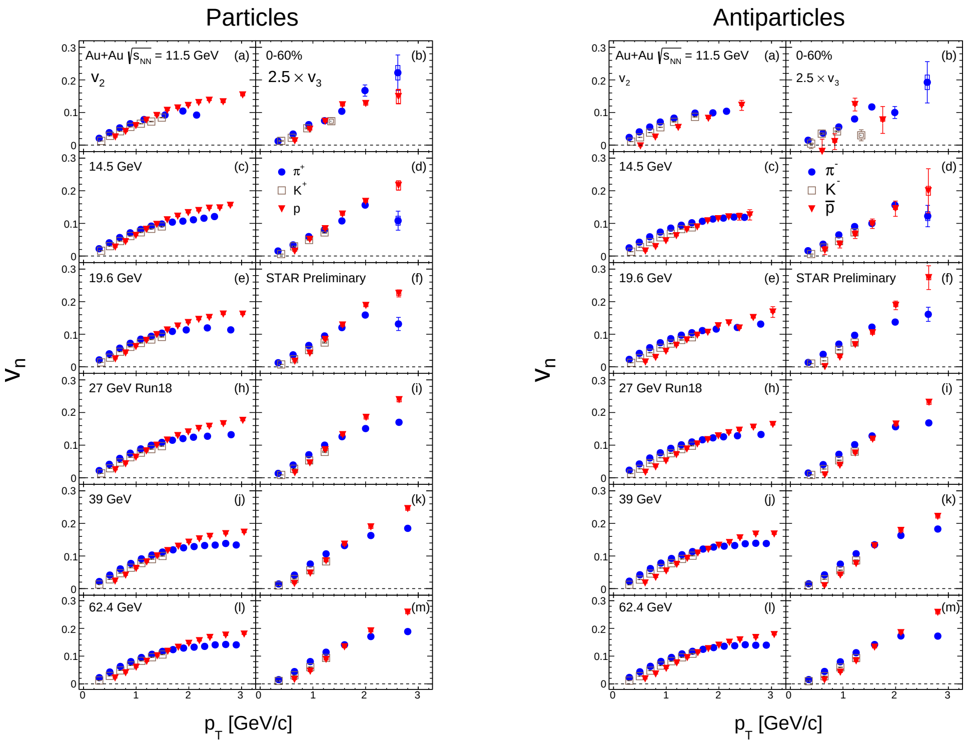

Figure 3. p_T dependence of v_2 and v_3 signals of π^+, K^+, p (left) and π^-, K^-, $\bar{p}$ (right) for 0-60% central Au+Au collisions.

Figure. 4 shows that the measured v_3 values of identified charged hadrons seems to follow the NCQ scaling, $v_n/n_q^{n/2}$ versus $(m_T - m_0)/n_q$, if we plot the results for particles (left part) and anti-particles (right part) separately.
The analysis of the new dataset of Au+Au collisions at $\sqrt{s_{NN}}$ = 27 GeV, collected by STAR experiment in 2018, allows us to observe the difference in the triangular v_3 flow between protons and anti-protons, see Fig. 5. It shows that, similar to elliptic flow v_2, the v_3 flow signal of protons is larger than v_3 of antiprotons and the difference has p_T dependence.

For other collision energies we can estimate the difference in v_3 values between particles and corresponding anti-particles for p_T-integrated v_3 values. The right part of Fig. 6 shows the difference in v_3 between particles (X) and their corresponding anti-particles ($\bar{X}$) as a function

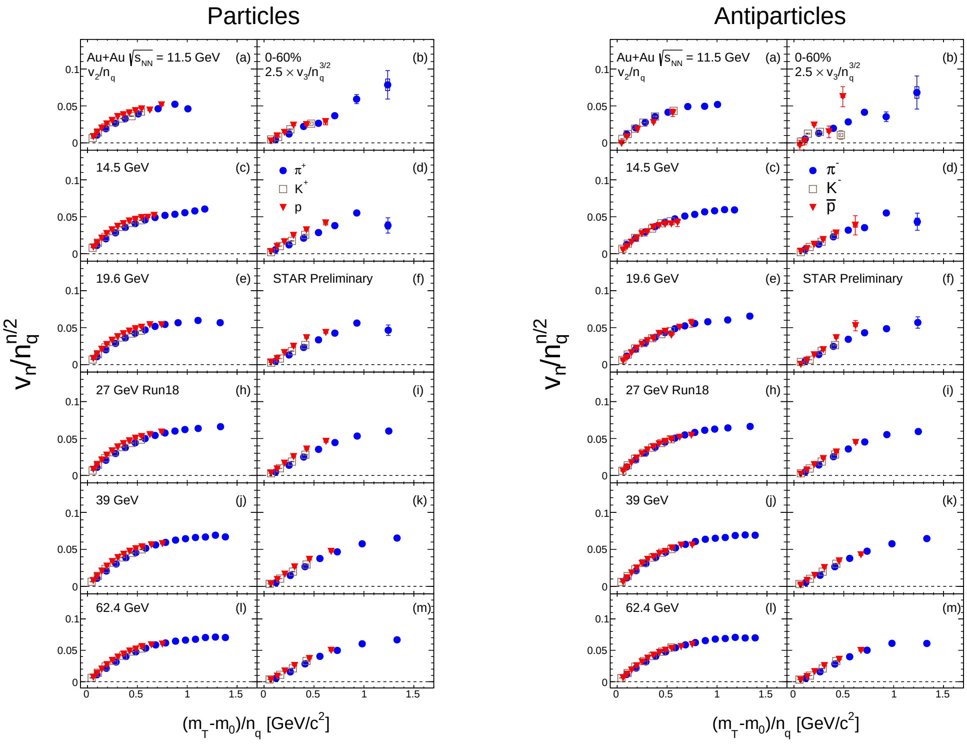

Figure 4. The Number-of-Constituent Quark (NCQ) scaled elliptic and triangular flow, $v_n/n_q^{n/2}$ versus $(m_T - m_0)/n_q$, for 0-60% central Au+Au collisions for for selected particles (left part) and corresponding anti-particles (right part).

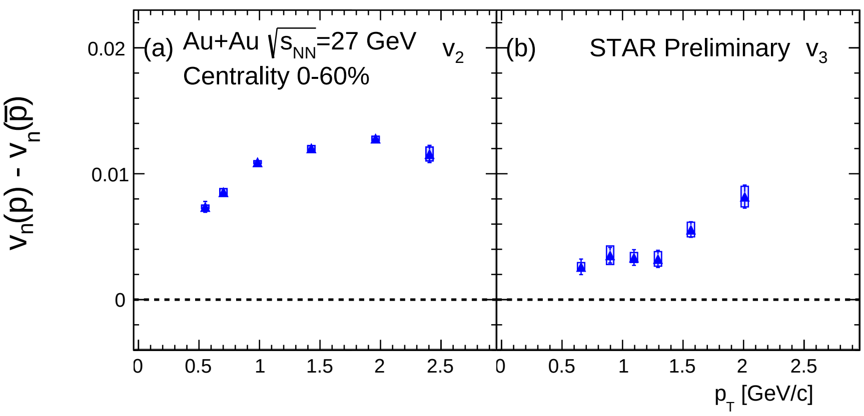

Figure 5. The difference between proton and antiproton v_n as a function of the transverse momentum p_T for 0-60% central Au+Au collisions at $\sqrt{s_{NN}} = 27$ GeV.

of $\sqrt{s_{NN}}$ for $0-60\%$ central Au+Au collisions. Similar to v_2, the $v_3(X) - v_3(\bar{X})$ difference increases with decreasing collision energy and it is larger for baryons than mesons [17, 18, 19].

4. Summary

In summary, we have employed the event plane method with η sub-events to carry out new measurements of the triangular (v_3) anisotropic flow coefficients for inclusive and identified charged hadrons ($\pi^{\pm}$, $K^{\pm}$, p, $\bar{p}$) at midrapidity in Au+Au collisions, spanning the collision

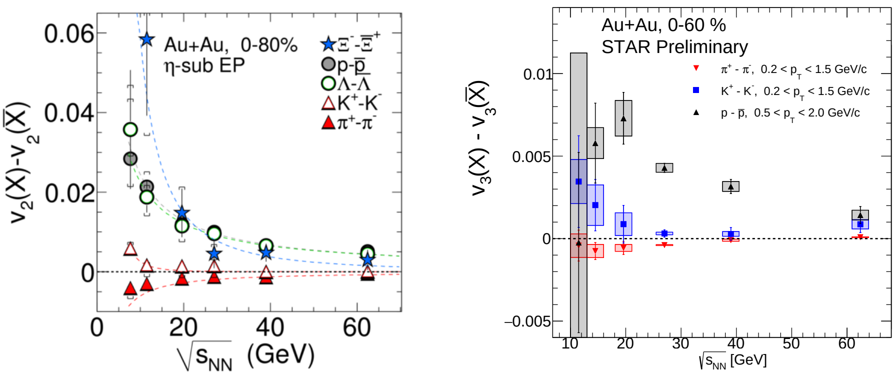

Figure 6. (left) The difference in v_2 between particles (X) and their corresponding anti-particles ($\bar{X}$) (see legend) as a function of $\sqrt{s_{NN}}$ for $0-80\%$ central Au+Au collisions. The figure is taken from [18]. (right) The preliminary results for the difference in the v_3 values between particles (X) and its corresponding anti-particles ($\bar{X}$) as a function of $\sqrt{s_{NN}}$ for 0-60% central Au+Au collisions.

energy range $\sqrt{s_{NN}}$ = 11.5 - 62.4 GeV. We observe that the triangular flow signal (v_3) of identified hadrons exhibits similar trends as first observed for v_2 [16, 17, 18]. New measurements of v_3 excitation function could serve as constraints to test different models and to aid new information about the temperature dependence of the transport properties of the strongly interacting matter.

5. Acknowledgments

This work is supported by the RFBR according to the research project No. 18-02-40086 and by the Ministry of Science and Higher Education of the Russian Federation, Project "Fundamental properties of elementary particles and cosmology" No 0723-2020-0041.

References

[1] J. Adams *et al.* [STAR Collaboration], Nucl. Phys. A **757** (2005) 102
[2] K. Adcox *et al.* [PHENIX Collaboration], Nucl. Phys. A **757** (2005) 184
[3] J. E. Bernhard, J. S. Moreland and S. A. Bass, Nature Phys. **15** (2019) no.11, 1113-1117
[4] Y. Aoki, G. Endrodi, Z. Fodor, S. D. Katz and K. K. Szabo, Nature **443** (2006) 675
[5] D. Keane, J. Phys. Conf. Ser. **878** (2017) no.1, 012015.
[6] H. Caines, Nucl. Phys. A **967** (2017) 121.
[7] S. A. Voloshin, A. M. Poskanzer and R. Snellings, Landolt-Bornstein **23** (2010), 293-333
[8] R. Snellings, J. Phys. G **41** (2014) no.12, 124007
[9] S. Voloshin and Y. Zhang, Z. Phys. C **70** (1996) 665
[10] A. Adare *et al.* [PHENIX], Phys. Rev. C **93** (2016) no.5, 051902
[11] L. Adamczyk *et al.* [STAR], Phys. Rev. C **98** (2018) no.1, 014915
[12] J. Adam *et al.* [ALICE], JHEP **09** (2016), 164
[13] B. Schenke, S. Jeon and C. Gale, Phys. Rev. Lett. **106** (2011), 042301
[14] J. Auvinen and H. Petersen, Phys. Rev. C **88** (2013) no.6, 064908
[15] L. Adamczyk *et al.* [STAR], Phys. Rev. Lett. **118** (2017) no.21, 212301
[16] L. Adamczyk *et al.* [STAR], Phys. Rev. C **86**, 054908 (2012)
[17] L. Adamczyk *et al.* [STAR], Phys. Rev. C **88**, 014902 (2013)
[18] L. Adamczyk *et al.* [STAR], Phys. Rev. Lett. **110** (2013) no.14, 142301
[19] L. Adamczyk *et al.* [STAR], Phys. Rev. C **93**, no.1, 014907 (2016)
[20] L. Adamczyk *et al.* [STAR], Phys. Rev. Lett. **116** (2016) no.11, 112302
[21] G. Torrieri, Eur. Phys. J. A **52** (2016) no.8, 249